Giant Chiral Asymmetry in the C 1*s* Core Level Photoemission from Randomly Oriented Fenchone Enantiomers

Volker Ulrich,[†] Silko Barth,[†] Sanjeev Joshi,[†] and Uwe Hergenhahn[†]

Max-Planck-Institut für Plasmaphysik, EURATOM Association, Boltzmannstrasse 2, 85748 Garching, Germany

Elisabeth Mikajlo,[‡] Chris J. Harding,[§] and Ivan Powis*

School of Chemistry, The University of Nottingham, Nottingham NG7 2RD, UK

Received: October 5, 2007; In Final Form: December 20, 2007

Measurements made with a dilute, non-oriented, gas-phase sample of a selected fenchone enantiomer using circularly polarized synchrotron radiation demonstrate huge chiral asymmetries, approaching 20%, in the angular distribution of photoelectrons ejected from carbonyl C 1*s* core orbitals. This asymmetry in the forward−backward scattering of electrons along the direction of the incident soft X-ray radiation reverses when either the enantiomer or the left−right handedness of the light polarization is exchanged. Calculations are provided that model and explain the resulting photoelectron circular dichroism with quantitative accuracy up to ~7 eV above threshold. A discrepancy at higher energies is discussed in the light of a comparison with the closely related terpene, camphor. The photoelectron dichroism spectrum can be used to identify the absolute chiral configuration, and it is more effective at distinguishing the similar camphor and fenchone molecules than the corresponding core photoelectron spectrum.

Introduction

X-ray photoemission spectroscopy (XPS) is commonly recognized as element-specific molecular spectroscopy. Photoionization of the highly localized core levels is very atomic-like in nature, although variations in the valence electron density around the core site can produce chemical shifts in the core electron binding energies (CEBEs), of the order of a few percent, and these can be used to infer adjacent functional group structure of the molecule. The advent of high-intensity synchrotron radiation sources has added new possibilities, including the high resolution required for the observation of vibrational structure in gas-phase molecular XPS.[1] In this article, we wish to exploit another characteristic of current synchrotron X-ray sources, namely, their variable, high degree of polarization. Specifically, we describe the use of circularly polarized light (CPL) to observe photoelectron circular dichroism[2] (PECD) in the angle-resolved C 1*s* photoemission from randomly oriented, gas-phase enantiomers of fenchone. The asymmetry factors associated with this isolated molecule PECD are found to approach, under favorable experimental configurations, a figure of 20%, which is many orders of magnitude larger than that typically encountered in other chiroptical phenomena in the absence of orientation or cooperative enhancement effects in the solid state.[3]

Asymmetries of this magnitude were in fact predicted in the first quantitative calculations made for valence shell PECD,[4,5] and this expectation has been subsequently verified in a number of experimental studies made in the vacuum ultraviolet region.[6−9] The strength of this effect arises because it is present in the pure electric dipole approximation and so, unlike normal circular dichroism spectroscopy, it does not depend upon interactions involving much weaker magnetic dipole or electric quadrupole terms. Even so, it is perhaps a priori surprising that core electron ionization would show PECD of a similar magnitude, readily comparable to the valence shell results, given the localization of core orbitals and their generally weak response to the molecular environment. An initial 1*s* orbital is effectively achiral—spherically symmetric and localized—and as such is untouched by any chirality of the surrounding molecular structure. Nevertheless, PECD of a similar great magnitude has also been experimentally observed in C 1*s* photoemission.[10,11] Given an achiral initial orbital, it must be assumed that any observed chiral asymmetry in the photoelectron distribution is a consequence of the scattering of the outgoing photoelectron off the chiral molecular potential. The departing photoelectron thus provides an in-situ generated probe of the molecular structure.

There are strong indications from recent theoretical work[12,13] that the PECD carries an enhanced sensitivity to relatively small scattering terms and hence to changes in the molecular configuration; in the case of core ionization, this appears even when structural variations occur at some distance from the initial electron localization site. This indicates that for an enantiomeric sample a PECD measurement made using circular polarization may provide considerably enhanced sensitivity to the molecular structure compared to the usual linearly polarized XPS measurement—not only identifying the absolute chiral configuration, but possibly also shedding light on conformational subtleties. However, the prospect of conformational sensitivity is also a weakness while developing a basic understanding of the PECD effect, since rarely is the relative population of different conformers of a floppy molecule accurately known

* Corresponding author. Tel: +44 115 9513467. Fax: +44 115 9513562. E-mail: ivan.powis@nottingham.ac.uk.

[†] Mail address: c/o BESSY mbH, Albert-Einstein-Str. 15, 12489 Berlin, Germany.

[‡] Current address: Defence Science and Technology Organisation, Bldg 307 EOP, P.O. Box 1500, Edinburgh, South Australia 5111.

[§] Current address: Lehrstuhl für Physikalische Chemie 1, Technische Universität München, Lichtenbergstrasse 4, 85748 Garching, Germany.

10.1021/jp709761u CCC: $40.75
Published on Web 03/21/2008

under specific experimental conditions, with some resulting ambiguity when interpreting results.

For this reason, the rigid bicyclic structure of fenchone offers some certainty when a comparison of theory and experiment is attempted, making it attractive for our studies. At the same time, it should prove possible to examine whether PECD does offer enhanced structure information by comparing results obtained for fenchone with those previously reported for C 1*s* ionization of the equally rigid camphor.[10] These two terpenes differ only in the substitution site of two methyl groups.

Quite generally, the normalized photoelectron angular distribution expected in single photon ionization can be written as[5]

$$I_p(\theta) = 1 + b_1{}^p P_1(\cos\theta) + b_2{}^p P_2(\cos\theta) \qquad (1)$$

where P_n is a Legendre polynomial of order n, and the coefficients $b_n{}^p$ depend on the polarization, p, of the ionizing radiation. For linearly polarized light ($p = 0$), the first angular coefficient, $b_1{}^0$, is always zero and the familiar $\cos^2$ form of the non-isotropic part of the angular distribution function is recovered from just the second Legendre polynomial term (where $b_2{}^0 \equiv \beta$). Here, the angle θ is measured with respect to the linear polarization direction. This absence of any contribution from the P_1 term also rigorously applies for any achiral molecule. However, for circularly polarized radiation ($p = \pm 1$) and a chiral molecule, the coefficients $b_1{}^{\pm 1}$ can be expected to be nonzero, such that the angular distribution now acquires an additional $\cos\theta$ dependence from the first Legendre polynomial term. In this case, θ defines the electron direction relative to the photon beam propagation, so that for a given circular polarization and a given molecular enantiomer eq 1 describes a forward−backward asymmetry in the electron angular distribution along the light beam. A quantitative measure of this angular asymmetry for a given enantiomer and light helicity, p, can be defined from eq 1 as the difference in the electron fluxes through equal area elements on the unit sphere in the 0° and 180° directions normalized to the mean flux through an area element (average over the whole sphere):

$$G_{\mathrm{AD}} = \left| \frac{I_p(0°)\sin\theta\,\mathrm{d}\theta\,\mathrm{d}\varphi - I_p(180°)\sin\theta\,\mathrm{d}\theta\,\mathrm{d}\varphi}{\sin\theta\,\mathrm{d}\theta\,\mathrm{d}\varphi} \right| = 2b_1{}^p \qquad (2)$$

where the expression has been simplified making use of the properties of the Legendre polynomials.

Further examination[5] of the $b_1{}^{\pm 1}$ coefficients reveals their antisymmetry; they change sign with either an exchange of molecular enantiomer or with a switch from left to right CPL ($p = +1 \leftrightarrow p = -1$). This latter property generates a circular dichroism that is observable, for a given enantiomer and at a given detector angle, by switching polarization. We can then define a corresponding asymmetry for the dichroism as

$$\Gamma_0 = (I_{+1}(0°) - I_{-1}(0°)) = -(I_{+1}(180°) - I_{-1}(180°)) = \frac{(I_{+1}(\theta) - I_{-1}(\theta))}{\cos\theta} = 2b_1{}^{\{+1\}} \qquad (3)$$

where we have also made use of the symmetry properties of the P_2 term coefficients,[5] $b_2{}^{+1} = b_2{}^{-1}$ ($= -(1/2)b_2{}^0$), to eliminate them from the final expression.

Clearly these asymmetry definitions provide equivalent access to the $b_1{}^{\pm 1}$ angular distribution parameters, which can be the object of theoretical modeling. Photoelectron imaging experiments that observe the full 4π angular distribution can either provide directly the asymmetry in the angular distribution, eq 2, or where alternate left and right circular polarization states are available a dichroism measurement, such as suggested by eq 3.[6,7] However, when convenient polarization switching is possible, a dispersive analyzer mounted at some single fixed angle, θ, to the light beam provides an alternative means to observe PECD, and this approach has been adopted to measure the PECD and the $b_1{}^{+1}$ coefficient in the present study.

Experimental and Computational Details

Experiments took place, on a number of separate occasions, on the UE56/2 soft X-ray beamline at the BESSY-II synchrotron (Berlin). This dual undulator beamline has a facility for rapid polarization switching, which proves to be of great value in minimizing apparatus asymmetries because of, for example, sample pressure variations. The spectrometer, a single Scienta SES 200 hemispherical analyzer, was mounted at a forward scattering angle of 54.7° from the horizontal beam direction. Commercial samples of the 1R,4S (-) [Aldrich, 98%] and 1S,-4R (+) [Fluka 99.5%] fenchone enantiomers were placed, without further purification, in a small reservoir connected to the gas ionization cell. Gentle heating (50−80 °C) was applied to the reservoir, transfer lines, and gas cell to raise the vapor pressure in the ionization region to an estimated 5×10^{-5} mbar. With our current gas cell design, this led to a sample consumption of ≤50 mg per measurement. A fuller account of the experiment and methodology adopted has been given previously, particularly a detailed account of the data recording that is designed to minimize any possible instrumental contributions to the asymmetry.[11]

An experimental asymmetry is obtained as the difference over the mean of two spectral intensities, S_p, recorded with left and right CPL at the fixed angle, θ:

$$\Gamma(\theta) = \frac{S_{+1} - S_{-1}}{\langle S_{\pm 1}\rangle} = \frac{N_{+1}I_{+1}(\theta) - N_{-1}I_{-1}(\theta)}{\langle N_{\pm}I_{\pm}(\theta)\rangle} \equiv \frac{2b_1{}^{+1}(\cos\theta)}{(1 + b_2{}^{\pm 1}P_2(\cos\theta))} \qquad (4)$$

where for the second step we have assumed that the recorded electron count can be expressed as a total ionization rate, N_p, times an appropriate angular function, $I_p(\theta)$. Experimentally it is arranged[11] that $N_{+1} = N_{-1}$ so that the rates cancel out in this expression for $\Gamma(\theta)$; then by assuming the electric-dipole angular distribution expression (eq 1), the equivalence that appears as the final step in eq 4 can be demonstrated. This general result for the experimental asymmetry suggests the need for a two-parameter fit for the theoretical coefficients $b_2{}^{\pm 1}$ and $b_1{}^{+1}$, but this may be circumvented by the choice of $\theta = 54.7°$, the magic angle at which the second Legendre polynomial term has a value of zero, effectively eliminating any dependence on the $b_2{}^{\pm 1}$ coefficient in eq 4. We therefore obtain

$$\Gamma(54.7°) \equiv 2b_1{}^{+1}(\cos 54.7°) \qquad (5)$$

which, apart from the cos 54.7° makes our experimental dichroism measurement equivalent to either G_{AD} (eq 2) or Γ_0 (eq 3) in yielding the chiral $b_1{}^{+1}$ parameter.

Calculations to provide theoretical photoionization parameters, including the chiral $b_1{}^{\pm 1}$ coefficients, were performed using the continuum multiple scattering model with an Xα local-exchange approximation (CMS−Xα) following procedures which have, again, been fully described previously.[5,12,14] Very briefly, a model potential is constructed using overlapping spherical

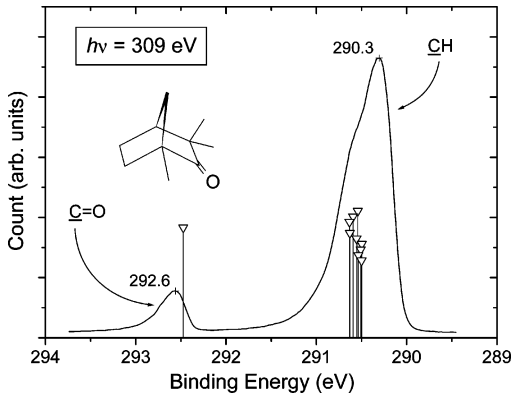

Figure 1. Fenchone XPS showing peak assignments. Calculated positions of C 1*s* core electron binding energies are also marked, with vertical offsets that are intended for clarity only.

regions placed at the atomic centers, these coordinates being obtained from an MP2/6-31G** optimized molecular geometry. The whole is placed in an outer spherical region, extending to infinity. The initial and continuum (ionized) states are then expanded using a spherical harmonic basis in each region, truncated at some value l_{max}. The photoionization electric dipole matrix elements are then evaluated, from which observable properties are calculated. The basis set l_{max} limits were systematically varied to ensure adequate convergence in both the convergence to self-consistency of the model potential and the calculated photoionization properties. The results reported here use, as a minimum, truncation limits for the neutral molecule calculations of 6/2/0 for (in order) the outer sphere/first row atoms/H atoms; for the continuum calculations these are increased to at least 18/10/3.

Results and Discussion

Figure 1 presents a fenchone XPS covering the carbon K-edge region. For this measurement the beamline slits were set to provide a photon bandwidth of ~40 meV, and the analyzer was operated with an estimated resolution of ~80 meV, giving a net resolution ~90 meV. Calibration of the spectrometer was made by measuring the known Xe Auger lines[15] and the CO_2 C $1s^{-1}$ band[16] at $h\nu = 310$ eV. The spectrum shows two distinct peaks that are fairly readily identified as the carbonyl C=O peak with a significant chemical shift from the remaining C atom centers. The assignment is verified with the aid of calculated binding energies obtained using Chong's ΔE_{KS}-(PW86−PW91)/cc_pCVTZ + C_{rel} method.[17,18] These calculated CEBEs are marked on the XPS and are seen to be in very close agreement with experiment. In particular, it strongly suggests that all the C 1*s* peaks other than the carbonyl one are strongly overlapping. Experimentally, there is no resolved structure in the major C−H_n peak other than a distinct shoulder at ~290.6 eV, which would be consistent with its having a composite nature.

PECD measurements were made with alternating circular polarization (0.1 Hz), as described previously.[11] While the high-resolution XPS (Figure 1) was recorded in scanning mode, the PECD spectra, S_p, were recorded in a fixed window mode, using a multichannel detector system to record simultaneously the complete region of interest. To capture the full fenchone C 1*s* spectrum required the use of a higher analyzer pass energy (75 eV) with consequent reduced resolution. The photon bandwidth was also increased to allow higher count rates, and the overall resolution now was estimated to be ~350 meV.

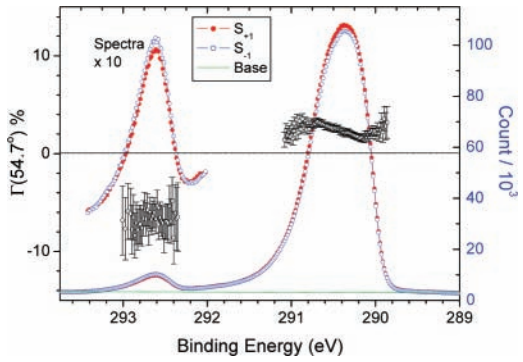

Figure 2. 1S-fenchone XPS at $h\nu = 298.6$ eV showing spectra recorded with left CPL (S_{+1}, positive photon helicity) and right CPL (S_{-1}, negative photon helicity). Also plotted on the figure are the asymmetries, Γ(54.7°), obtained as the difference divided by the mean of S_{+1} and S_{-1}, together with associated estimated error bars.

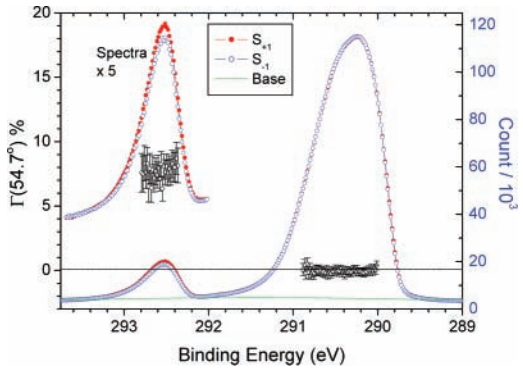

Figure 3. 1R-fenchone C 1*s* XPS recorded at $h\nu = 301.6$ eV. Other details are as for Figure 2.

Figure 2 shows an example of the 1S-fenchone enantiomer spectra recorded with left and right CPL, after careful treatment to eliminate instrumental differences. Differences between the peak intensities recorded with the alternate polarizations are clearly visible, and the differences, $S_{+1} - S_{-1}$, are presented as the raw asymmetry, Γ(54.7°), after normalizing to the mean count, $\langle S_{\pm 1} \rangle$. In this instance the main C−H peak is seen to have a small positive asymmetry, the C=O peak a larger negative asymmetry averaging around −7.5%. After allowance for the cos(54.7°) factor, this suggests for the C=O peak a magnitude for $2|b_1^{+1}|$, and hence the forward−backward asymmetry parallel to the photon beam (G_{AD}, eq 2) of 13%.

A second example, recorded this time for the 1R-enantiomer at 301.6 eV is shown in Figure 3. The C=O peak has a similar magnitude asymmetry, though of opposite sign, whereas the C−H peak at this photon energy has no perceptible asymmetry. This is in fact a more typical finding for the C−H peak. We have argued previously from the analogous observation in camphor PECD that in such composite peaks, each individual orbital ionization may have a significant nonzero PECD of either sign, but that on averaging over all components of the peak this would reduce toward a zero net asymmetry.[10] In any case, a full interpretation of the C−H peak asymmetry would be very difficult, given the large number of overlapping orbital contributions and the lack of knowledge about their relative weightings (cross sections). Consequently, we henceforth focus our attention on the well-resolved and characterized C=O peak asymmetries.

In Figure 4 we show the 1R-enantiomer C=O peak spectra (S_{+1}, S_{-1}) recorded at an intermediate photon energy. The raw asymmetry, Γ(54.7°) is now seen to be about 10.5%, from which

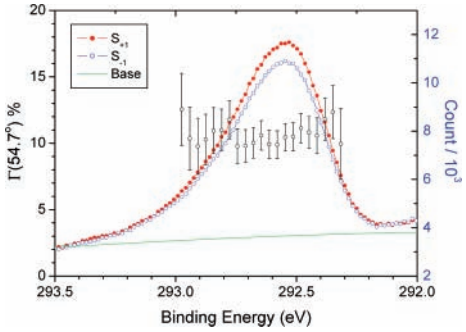

Figure 4. 1R-fenchone C=O 1*s* XPS recorded at photon energy $h\nu = 300.1$ eV. Other details as for Figure 2.

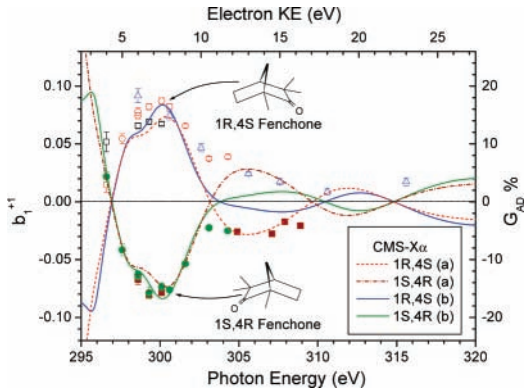

Figure 5. Chiral b_1^{+1} values and the corresponding predicted angular asymmetry factors, G_{AD}, for fenchone C=O $1s^{-1}$ photoionization. Open plotting symbols are for the 1R-, filled symbols are for the 1S-enantiomer data. In each set the different symbol shapes indicate measurements made on separate experimental occasions. Curves are plotted to indicate the results obtained from two variants of the CMS−Xα calculation, (a) and (b), as discussed in the text.

we may infer a corresponding forward−backward scattering asymmetry, G_{AD}, of ~18%. In fact, this asymmetry remains effectively constant across the band to within the estimated statistical error limits, though there is evidence from some measurements made at other photon energies to suggest that more systematic variations may occur under certain circumstances. If so, these might be associated with vibronic changes across the width of the band, though currently there are no appropriate theoretical treatments for such cases.

To study more closely the energy and enantiomer dependence of the PECD, we extract the mean asymmetries across the fwhm of each of the measured C=O XPS peaks. These are then scaled to correct for the measured degree of circular polarization[11] (which varies slightly with photon energy) and experimental b_1^{+1} values are deduced after division by 2 cos(54.7°) (eq 5) permitting a direct comparison with theoretical estimates for these chiral coefficients. These results are presented in Figure 5. Measurements for each enantiomer pair were completed across two separate beamtimes (with additional 1R-enantiomer data from a third period also), and some overlapping measurements were made to check reproducibility. This seems to be good, as there are no major discrepancies between data acquired on separate occasions.

First, it is seen from Figure 5 that the experimental 1R- and 1S-enantiomer trends mirror one another, essentially perfectly, differing in sign but sharing the same magnitude as a function of photon energy. This mirroring, or antisymmetry, of the b_1^1 coefficients for the two opposite handed enantiomers is fully to be expected from the theoretical treatment underpinning eq 1. From an experimental point of view, it clearly demonstrates a molecular origin for the observed asymmetries, since it is only the enantiomer that has changed.

The asymmetry peaks near 300 eV at $|b_1^{+1}| \approx 9\%$, or a corresponding forward−backward asymmetry $|G_{AD}| \approx 18\%$. Compared to, for example, electronic circular dichroism in total absorption, where asymmetries of $10^{-5}-10^{-4}$ are usual, this differential (i.e., angle-resolved) dichroism measurement thus yields asymmetries of enormous magnitude. This is immediately obvious from the very visible differences between the left and right CPL XPS spectra in, for example, Figure 4.

Theoretical CMS−Xα calculations giving b_1^{+1} coefficients for each enantiomer are included for comparison in Figure 5. In the region below $h\nu = 303$ eV, the preliminary calculations, labeled (a), produce good agreement with experiment. The curve for a given enantiomer clearly predicts the correct sign of the major region of chiral asymmetry, so that absolute configuration could have been assigned from these results. Between $h\nu = 303$ eV and $h\nu = 309$ eV, however, while the experimental asymmetry decreases, the calculation undershoots, the 1R-enantiomer curve, for example, becoming negative in contrast to the experiment remaining positive. Above this energy, the indications are that reasonable agreement is restored.

One aspect of the CMS−Xα calculation is the semiempirical nature of the molecular potential used. Part of the parametrization process involves assigning radii to the atomic sphere regions. We started (a) with an unbiased choice using optimized H, C, and O values suggested by Takai and Johnson.[19] In seeking more understanding of the discrepancy noted at 306 eV, an alternative recommendation for the H atom radius[20] has also been investigated. The results of this are included as modified CMS−Xα curves (b) in Figure 5. An unwanted consequence of this change is that the potential becomes overall too attractive (as judged from the shift in core level eigenvalues and the continuum features). This problem of capturing the exact binding energy with a model potential is not unique to CMS−Xα calculations, and experienced in other, more sophisticated, DFT-based methods too.[14] An ad hoc resolution is achieved by offsetting the energy scale on plotted curves—in this case by +0.75 eV. With this energy scale correction, the agreement with experiment below $h\nu = 303$ eV is seen to be even better, but the undershoot around 306 eV, while reduced, still proves a discrepancy.

Finally, the effect of enlarging the H atom angular basis set beyond a minimal ($l = 0$) has been explored. Adopting a neutral molecule 6/2/1 basis (using the earlier notation) has the principal benefit of removing the need for the ad hoc energy scale adjustment that was necessitated following the adoption of smaller H atom sphere sizes. Combining these changes with a similarly enlarged 18/10/5 continuum state basis produces small benefits in the overall quality of the b_1^{+1} parameter fit with experiment, and it is shown in Figure 6 as CMS−Xα calculation (c). Any further increase in basis set size produces negligible changes. All these calculations have also been re-run for an alternative B3LYP/6-31G** optimized geometry, but without finding that any significant changes result.

In performing all these CMS−Xα calculations, the full molecular angular basis is used for computing the initial C 1*s* state, which therefore allows for mixing and polarization of the nominally spherical 1*s* orbital in the molecular environment. Nevertheless, in this model the orbital retains >99% localized *s* character, with a similar result found in Hartree−Fock calculations with a 6-31G(p,d) basis. Even though these results

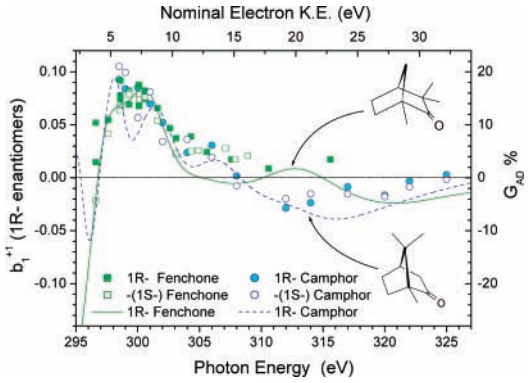

Figure 6. Carbonyl C $1s^{-1}$ PECD data for fenchone and camphor (ref 10). For both molecules the negatives of the 1S-enantiomer data are plotted for direct comparison with the 1R-enantiomer data. Comparisons are offered with 1R-enantiomer CMS−Xα calculations for fenchone [variant (c) - modified small H-spheres, 6/2/1 neutral basis, 18/10/5 continuum basis] and camphor (taken from refs 7 and 14).

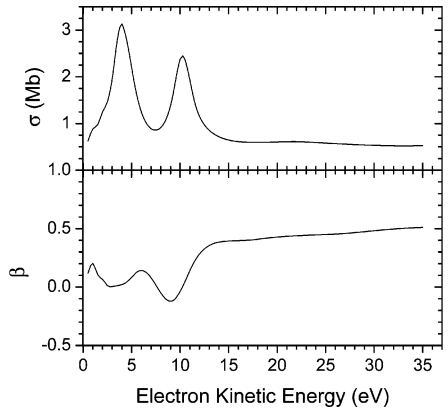

Figure 7. CMS−Xα cross section, σ, and anisotropy parameter β ($\equiv b_2^0 = -2 \times b_2^{\pm 1}$) for the fenchone carbonyl C $1s^{-1}$ photoionization.

suggest there is only minimal non-spherical distortion of the initial orbital, it is worthwhile examining how much this may contribute to the observed chiral photoelectron angular distribution. The previous CMS−Xα calculations were therefore repeated with the angular basis of the initial orbital constrained as a single pure *s* function located on the carbonyl carbon center. The computed angular distribution parameters were found to be imperceptibly changed by this constraint. The large chiral effects which have been observed in this system therefore persist even with an enforced fully achiral (spherical) initial state and so here, at least, the PECD must result overwhelmingly as a consequence of final-state scattering of the emitted electron by the chiral molecular potential.

It is of interest at this point to introduce a comparison with the C $1s^{-1}$ photoionization of the very closely related molecule camphor.[10,21] The simple C *K*-edge XPS of these two molecules are virtually identical, as can be seen comparing Figure 1 of this paper and Figure 5 in ref 21, and, despite very small differences in CEBE shifts, do not discriminate between the two. In Figure 6, we compare the PECD results for camphor[10] and fenchone. To do so, results for both molecules are placed on the same plot, and to further compact the data the S-enantiomer b_1^{+1} values for either molecule are negated before plotting to bring them onto the same trend lines as their R-enantiomer counterparts.

At photon energies up to 306 eV the experimental camphor and fenchone PECD results in Figure 6 are seen to be indistinguishable, to within the likely experimental error. However, above this photon energy there is clear indication of divergent behavior, the camphor 1R- (1S-) b_1^{+1} values crossing the axis and becoming negative (positive), while the sign of the fenchone data remains unaltered. This behavior for camphor is well replicated in the theoretical treatments,[14] whereas for fenchone, as already noted, agreement worsens above 303 eV. However, just as experiments for the two molecular species diverge at the higher photon energies, so do the associated CMS−Xα calculations. Comparing the molecular structures that are sketched in Figure 6, it can be seen that the significant change between fenchone and camphor is a "migration" of two methyl substituent groups from an α- to a β- site, in the latter case with the asymmetric carbon interposed. From the similarity of the pure XPS results it would appear that the electron density surrounding the carbonyl carbon (and so the initial carbonyl C 1*s* orbital) is scarcely affected by this change. The predicted, and actual, differences in the chiral photoelectron angular distributions must then be associated with a final-state photoelectron scattering off the changed regions of the molecule, becoming apparent for electron kinetic energies of 10 eV or more.

In an earlier theoretical study of the camphor molecule PECD, Stener et al.[14] identified resonance-like structures at electron kinetic energies of ∼4, 10.6, and more weakly at 21.3 eV. The calculated cross section and β-parameter for the fenchone carbonyl C 1*s* ionization (Figure 7) are very similar to those obtained for camphor (see Figure 1, ref 14), with the same characteristic features being evident. In particular, the 10 eV structure in camphor was identified by examination of the B-spline continuum function as a shape resonance resembling a localized CO σ^* virtual valence orbital,[14] and it is not unreasonable to suppose a similar explanation for the 10 eV feature in fenchone. This most pronounced feature in the fenchone continuum coincides, however, with the region where theory and experiment for the fenchone b_1^{+1} coefficient diverge—an electron kinetic energy of 10 eV for the carbonyl ionization corresponding to a photon energy of 303 eV. It may thus be inferred that while the low-energy region is well accounted for by theoretical modeling, the difficulties noted at $h\nu = 303$ eV indicate that reliable treatment in the vicinity of a shape resonance remains a challenge for theory. Resonance-induced continuum phase shifts are normally expected to strongly influence photoelectron angular distributions, but it has been pointed out[13] that chiral $b_1^{\pm 1}$ parameters seem to be at least as sensitive to tiny potential asymmetries, possibly masking any simple correlation between the resonance and structure in the PECD curves.

Conclusions

The measurements that have been made here demonstrate an enormous chiral asymmetry effect (approaching 20%) that is several powers of ten greater than most other demonstrated chiroptical effects and within 1 order of magnitude of the maximum conceivable asymmetry of 100%! The effect is apparent even from visual examination of the raw data, yet this is obtained from inherently dilute, non-oriented, non-interacting molecules. There is obvious scope for exploiting this as a sensitive chiral tool.

The observed asymmetry comes about as the emerging photoelectron probes the chiral molecular potential, the handedness of which is clearly related to the configuration of the nuclei in the molecule. A 1*s* core orbital is localized and effectively spherical, so does not experience the molecular chirality; PECD in these cases is very much a final-state scattering effect.

The comparisons that we have here been able to make between fenchone and the very closely similar molecule camphor are revealing. The localized nature of the C 1*s* orbitals and the evidently similar distribution of valence electron density about these sites means that the carbon *K*-edge photoelectron spectra are virtually identical and so do not discriminate between these species. On the other hand, measurement of just the carbonyl C 1*s* electron angular distributions made with circularly polarized radiation—either made as a dichroism measurement with alternating left−right polarization or as a full measurement of the laboratory frame angular distribution function—have some capability to distinguish the two in an appropriate kinetic energy range. Perhaps more significantly, these PECD measurements clearly have the ability to distinguish the handedness of an enantiomeric sample. Generally speaking, the overall evidence now suggests that current calculations for C 1*s* ionizations are sufficiently reliable that the absolute configuration could be confidently inferred.[10−12,14] When agreement between experiment and a theoretical prediction is demonstrated, as done here for the dominant region of the PECD spectrum up to a kinetic energy ∼10 eV, it can be almost quantitatively exact. Of course, in the example of fenchone, discrepancies are seen at some slightly higher electron energies, but viewed in the context of the full range studied these intermediate regions are clearly seen as anomalous. Comparison with previous camphor studies[14] suggests why these particular difficulties might arise.

Acknowledgment. The authors thank the technical staff of BESSY for support and assistance. This work was supported by the European Community - Research Infrastructure Action under the FP6 "Structuring the European Research Area" Programme. The calculations were in part facilitated by the provision of resources by the EPSRC National Service for Computational Chemistry Software.

References and Notes

(1) Hergenhahn, U. *J. Phys. B: At. Mol. Opt. Phys.* **2004**, *37*, R89.

(2) Powis, I. Photoelectron Circular Dichroism in Chiral Molecules. In *Adv. Chem. Phys.*; Light, J. C., Ed.; Wiley: New York, 2008; Vol. 138; pp 267−329.

(3) Barron, L. D. *Molecular light scattering and optical activity*, 2nd ed.; Cambridge University Press: Cambridge, 2004.

(4) Powis, I. *J. Phys. Chem. A* **2000**, *104*, 878.

(5) Powis, I. *J. Chem. Phys.* **2000**, *112*, 301.

(6) Garcia, G. A.; Nahon, L.; Lebech, M.; Houver, J. C.; Dowek, D.; Powis, I. *J. Chem. Phys.* **2003**, *119*, 8781.

(7) Nahon, L.; Garcia, G. A.; Harding, C. J.; Mikajlo, E. A.; Powis, I. *J. Chem. Phys.* **2006**, *125*, 114309.

(8) Stranges, S.; Turchini, S.; Alagia, M.; Alberti, G.; Contini, G.; Decleva, P.; Fronzoni, G.; Stener, M.; Zema, N.; Prosperi, T. *J. Chem. Phys.* **2005**, *122*, 244303. Giardini, A.; Catone, D.; Stranges, S.; Satta, M.; Tacconi, M.; Piccirillo, S.; Turchini, S.; Zema, N.; Contini, G.; Prosperi, T.; Decleva, P.; Di Tommaso, D.; Fronzoni, G.; Stener, M.; Filippi, A.; Speranza, M. *ChemPhysChem* **2005**, *6*, 1164.

(9) Lischke, T.; Böwering, N.; Schmidtke, B.; Müller, N.; Khalil, T.; Heinzmann, U. *Phys. Rev. A* **2004**, *70*, 022507.

(10) Hergenhahn, U.; Rennie, E. E.; Kugeler, O.; Marburger, S.; Lischke, T.; Powis, I.; Garcia, G. *J. Chem. Phys.* **2004**, *120*, 4553.

(11) Harding, C. J.; Mikajlo, E. A.; Powis, I.; Barth, S.; Joshi, S.; Ulrich, V.; Hergenhahn, U. *J. Chem. Phys.* **2005**, *123*, 234310.

(12) Harding, C. J.; Powis, I. *J. Chem. Phys.* **2006**, *125*, 234306.

(13) Di Tommaso, D.; Stener, M.; Fronzoni, G.; Decleva, P. *ChemPhysChem* **2006**, *7*, 924.

(14) Stener, M.; Tommaso, D. D.; Fronzoni, G.; Decleva, P.; Powis, I. *J. Chem. Phys.* **2006**, *124*, 024326.

(15) Carroll, T. X.; Bozek, J. D.; Kukk, E.; Myrseth, V.; Saethre, L. J.; Thomas, T. D.; Wiesner, K. *J. Electron Spectrosc. Relat. Phenom.* **2002**, *125*, 127.

(16) Myrseth, V.; Bozek, J. D.; Kukk, E.; Saethre, L. J.; Thomas, T. D. *J. Electron Spectrosc. Relat. Phenom.* **2002**, *122*, 57.

(17) Takahata, Y.; Chong, D. P. *J. Electron Spectrosc. Relat. Phenom.* **2003**, *133*, 69.

(18) Cavigliasso, G.; Chong, D. P. *J. Chem. Phys.* **1999**, *111*, 9485.

(19) Takai, Y.; Johnson, K. H. *Chem. Phys. Lett.* **1992**, *189*, 518.

(20) Takai, Y.; Donovan, M. M.; Johnson, K. H.; Kalonji, G. *Chem. Phys. Lett.* **1989**, *159*, 376.

(21) Rennie, E. E.; Powis, I.; Hergenhahn, U.; Kugeler, O.; Garcia, G.; Lischke, T.; Marburger, S. *J Electron Spectrosc. Relat. Phenom.* **2002**, *125*, 197.